

## A pulse plating method for the electrosynthesis of ZnSe

M. BOUROUSHIAN\*, T. KOSANOVIC and N. SPYRELLIS

*General Chemistry Laboratory, Chemical Engineering School, National Technical University of Athens, 9 Iroon Polytechniou str., Zografos Campus, 157 73, Athens, Greece*

(\*author for correspondence, tel.: + 30-210-7723097, fax: + 30-210-7723088, e-mail: mirtatb@central.ntua.gr)

Received 15 August 2005; accepted in revised form 7 March 2006

**Key words:** aqueous electrochemistry, pulse electrodeposition, thin film chalcogenides, voltammetry, X-ray diffraction, zinc selenide

### Abstract

Polycrystalline, thin films of ZnSe semiconductor compound were formed by cathodic electrodeposition from acidic aqueous selenite solutions of zinc sulphate, by using a potentiodynamic technique involving the application of repeated double pulses of controlled potential. Conditions for obtaining coherently uniform deposits with enhanced ZnSe to Se ratios were specified, on the basis of X-ray diffraction (XRD) and scanning electron microscopy results, by investigating the combined effect of the potential and length of each pulse as determined by duty cycle and frequency. It was shown that pulse plating process is a viable alternative to potentiostatic electrodeposition allowing improved control of the solid phase composition.

### 1. Introduction

Zinc selenide is a refractory material applicable in electronic and optoelectronic devices as being a semiconductor with a direct, wide band gap of 2.7 eV. Since conventional crystallization of ZnSe from the melt is not expedient because of its high melting point (1526 °C), various methods have been used for the synthesis of single crystal or polycrystalline ZnSe films, including molecular beam epitaxy [1], chemical vapor deposition [2], organometallic chemical vapor deposition [3], and electrocrystallization from molten salts, aqueous or non-aqueous solutions [4–11]. The development of soft chemistry methods for synthesizing ZnSe is of particular interest. Aqueous electrodeposition is relatively simple, low-cost, and scaleable to large area. However the electrolytic fabrication of single phase and uniformly crystalline ZnSe films encounters the constraint of the large difference between the redox potentials of zinc and selenium precursor species, and the complex electrochemistry of selenium compounds.

Periodic pulse electrolysis (PPE) has been thoroughly treated theoretically and experimentally [12–14] as a powerful tool for innovative methods of electrodeposition. The main advantage over potentiostatic, direct current (DC) electrolysis is that PPE offers more independent variables so that a variety of mass transport situations and electrocrystallization conditions can be created for constant chemical composition of the bath. Pulse plating of metal coatings with improved properties, i.e. reduced porosity and impurity content as well as

increased adhesion and uniformity, has been formerly reported [12, 13, 15]. The application of PPE as an electrosynthetic route for the formation of alloys or binary ceramics is more complicated. Variants used for the formation of chalcogenides have been shown to promote improved composition control and reduction of film inhomogeneities. Stoichiometric and continuous films of CdTe have been produced by a pulse potential method [15] similar to that described here, while pulsed current methods with and without reversal, or pulsed potential with large pulse to pause ratios, led to CdTe, CdSe and CdSe<sub>x</sub>Te<sub>1-x</sub> layers with various microstructural features [16–18]. Reports on the pulse deposition of ZnSe are few: in evaluating various electroplating techniques, Natarajan et al. [4] remark that potentiostatic plating offers the best control of film composition.

Having investigated the electrocrystallization of ZnSe from acidic selenite solutions of Zn(II) under potentiostatic and galvanostatic conditions [8], we describe in this work experimental results of a PPE technique involving the application of double rectangular pulse potential waves.

### 2. Experimental details

The electrolysis setup consisted in a single compartment, thermostat-controlled three-electrode cell (Pt-grid counter and Hg/Hg<sub>2</sub>SO<sub>4</sub> saturated sulfate reference; SSE) fitted to a potentiostat system (Wenking PGS 81R) coupled to a pulse generator (Wenking DPC 72).

Rotating discs (12 mm-in-diameter) of commercial grade Ti or Ni were used as working electrodes (RDE; rotation rate 500 rpm). The pretreatment of the electrodes included abrasion and polishing by alumina powder (grain size  $0.3\ \mu\text{m}$ ). The Ti electrodes were etched by 10% HF for 10 s, in order to dissolve the surface oxide layer. Water (of  $18.3\ \text{M}\Omega\ \text{cm}^{-1}$ ) purified by an ultra-pure water system (Easy Pure Barnstead RF) and as-received analytical grade selenite ( $\text{SeO}_2$ ) and  $\text{ZnSO}_4 \cdot 7\text{H}_2\text{O}$  reagents were used.

The electrodeposition experiments were performed with aqueous solutions of  $0.01 \times 10^{-3}$ – $0.5 \times 10^{-3}$  M  $\text{SeO}_2$ , and 0.2 M  $\text{ZnSO}_4$ , buffered at  $\text{pH} = 2.5$ – $4$ , at  $85\ ^\circ\text{C}$ . The total electrolysis charge for each deposition was 5 C resulting in  $0.5$ – $1\ \mu\text{m}$ -thick films depending on their coherence. Deposition was carried out by imposing an alternating double signal of rectangular controlled potential with a specific duty cycle (d.c.) for each pulse and a time period ranging between 0.01 and 10 s. Several samples were submitted to heat treatment in a furnace controlled by a Shimaden FP21 programmable controller (heating rate:  $10\ ^\circ\text{C}\ \text{min}^{-1}$ ). Microstructural data were obtained by X-ray diffraction (XRD) in a Siemens D5000 unit with a  $\text{CuK}\alpha$  source, and by Scanning Electron Microscopy (SEM) in a JEOL JSM 6100 unit equipped with Energy dispersive X-ray local analysis (EDAX).

### 3. Results and discussion

#### 3.1. Voltammetry and pulse plating profiles

According to our previous research [8], a zinc blend phase of ZnSe could be formed electrolytically along with semi-metallic Se, as a result of the potentiostatic co-reduction of  $\text{Se}^{(+\text{IV})}$  species and  $\text{Zn}^{2+}$  ions or the homogeneous reaction between reduced  $\text{Se}^{-2}$  and  $\text{Zn}^{2+}$  in an acidic environment. Electrosynthesis was achieved using a large excess of  $\text{Zn}^{2+}$  in the electrolytic solution and adjusting the mass transfer in order to establish a chalcogen species diffusion-limited control of the process.

Cyclic voltammograms in  $0.05 \times 10^{-3}$  M  $\text{SeO}_2$ , 0.2 M  $\text{ZnSO}_4$ ,  $\text{pH} = 3$  electrolyte, including the background contributions to current, measured in open air as well as in oxygen-free acid solutions of similar ionic strength, are shown in Figure 1. A significant part of the diffusion current for the Ti electrode is associated to oxygen-related reactions; the reduction of hydrogen initiates at  $-1.3$  V (Figure 1, argon-deaerated bath). On the Ni electrode, the overpotential of hydrogen is lower and depolarization occurs at more positive potential. The zinc selenide compound, potentiostatically formed by underpotential reduction of  $\text{Zn}^{2+}$ , was detected at potentials as cathodic as  $-0.90$  V, though an appreciable amount of ZnSe crystallites is obtained only at potentials more negative than  $-1.15$  V (i.e. the onset of the diffusion plateau) up to  $-1.45$  V vs. SSE, the Nernst

potential of Zn. The reverse sweep in Figure 1 features the anodic stripping of the metal.

The electrodeposits produced by a potentiostatic process at potentials located in the diffusion plateau normally contain about 40 at.% crystalline Se [8] formed by direct reduction of  $\text{Se}^{(+\text{IV})}$  or precipitated after conproportionation with  $\text{Se}^{2-}$  produced on the cathode [4, 8]. A post deposition heat treatment drives off the excess, however building up a  $\text{Se}^{(0)}$  phase during growth constitutes a limiting factor for the crystallite size of ZnSe and the structural integrity of the film. In the present investigation, pulse plating was applied in order to refine the electrolytic film *during* growth. The general idea is that the formation of  $\text{Se}^{(0)}$  might be constrained according to the following consideration. In principle, at sufficiently cathodic potential  $\text{Zn}^{2+}$  and  $\text{Se}^{(+\text{IV})}$  are reduced to zero valency species (and/or to  $\text{Se}^{-2}$ ), simultaneously forming some ZnSe compound crystallites. A subsequent application of less cathodic potential partly strips the  $\text{Se}^{(0)}$  and  $\text{Zn}^{(0)}$  phases off the cathode while most nuclei of ZnSe, once formed, should be left unaffected or

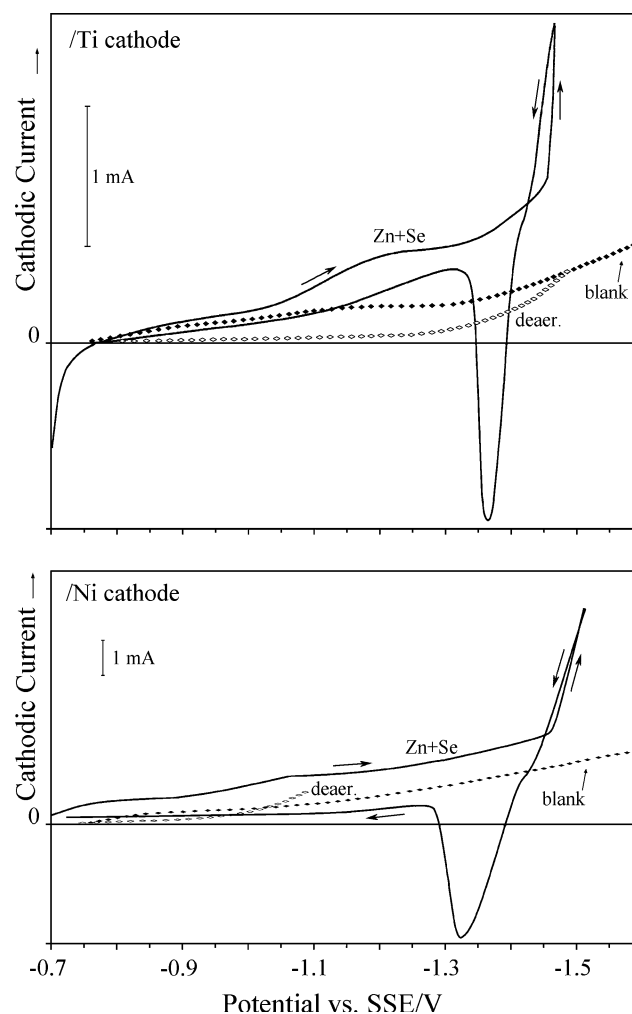


Fig. 1. Cathodic polarization of the Ti and Ni RDE (500 rpm, scan rate  $5\ \text{mV}\ \text{s}^{-1}$ ) at  $0.05 \times 10^{-3}$  M  $\text{SeO}_2$ , 0.2 M  $\text{ZnSO}_4$ ,  $\text{pH} = 3$  solution ("Zn + Se" curves). Background, "blank" curve recorded in  $\text{pH} = 3$  solution, 0.2 M in  $\text{K}_2\text{SO}_4$ ; "de aer." curve recorded in an argon-deaerated blank solution. The temperature is  $85\ ^\circ\text{C}$ .

grow further by the incorporation of constituent atoms, since the ZnSe phase has a largely negative free energy of formation ( $\Delta G_{298\text{K}} = -137\text{ kJ mol}^{-1}$ ). As a result, the periodic sequence of these steps progressively enriches the cathode surface with the compound.

Various combinations of potentials, duty cycles and frequencies were tested in order to determine an effective plating procedure. Each deposition cycle consisted of a double rectangular pulse of cathodic potential: one in the range  $-1.3$  to  $-1.8\text{ V}$ , and a less negative one located within the Zn underpotential range, i.e.  $-0.3$  to  $-1.4\text{ V}$ . Several configurations enabled deposition of coherent films containing relatively pure ZnSe crystallites. Functional cycles are shown in Figure 2 for different bath compositions. Both pulse potentials are reducing for  $\text{Se}^{(+\text{IV})}$ , while the charge flow reverses direction at a periodic time interval, resembling the pulsing current reversal technique.

### 3.2. Evaluation of the films electrodeposited under various potential profiles

The XRD response of as-grown ZnSe in most experimental conditions shows that the structure is crystalline, as illustrated in Figure 3a for a non-optimized electrodeposit. Well-resolved diffraction peaks of cubic blend ZnSe with random orientation of crystallites along the [111], [220] and [311] directions are observed, together with an admixture of hexagonal Se. The latter is easily removed either by heat treatment in air at temperatures

as low as  $200\text{ }^\circ\text{C}$  (Figure 3b) or by chemical etching with a suitable reagent (e.g. alkaline polysulphide solution).

The deposit constitutes an aggregate of spherical clusters and Se-rich forms (Figure 4a, 74% Se). After annealing the Zn to Se ratio is improved (Figure 4b, 57% Se) and a more cohesive and adherent layer is obtained, which optically resembles the characteristic yellowish colour of ZnSe. The remaining chalcogen excess is easily removed by further heating, while a well defined 1:1 stoichiometry can be directly established by processing at temperatures higher than  $350\text{ }^\circ\text{C}$  in an inert atmosphere [8]. The mild heating has a minor effect on the ZnSe crystallographic structure since the refractory compound stays unaffected at the relatively low temperatures employed.

The effect of aqueous  $\text{Se}^{(+\text{IV})}$  concentration on the properties of the deposited films was investigated for  $0.01 \times 10^{-3}$ ,  $0.05 \times 10^{-3}$  and  $0.5 \times 10^{-3}\text{ M}$   $\text{SeO}_2$  solutions (all  $0.2\text{ M}$  in  $\text{Zn}^{2+}$ ) and various pulse plating profiles. For constant electrical parameters (including total electrolysis charge), the quantity of the solid Se phase increased with the chalcogen content in the bath. Thus the lower  $\text{Se}^{(+\text{IV})}$  concentration gave lower excess of solid Se but the electrolysis time to achieving the desired charge was prohibitively long. On the other hand, although the films from  $0.05 \times 10^{-3}\text{ M}$   $\text{SeO}_2$  solutions contained lower Se excess than those obtained with  $0.5 \times 10^{-3}\text{ M}$   $\text{SeO}_2$ , the deposited ZnSe amount was not sensitive to the  $\text{Se}^{(+\text{IV})}$  concentration within this one order of magnitude.

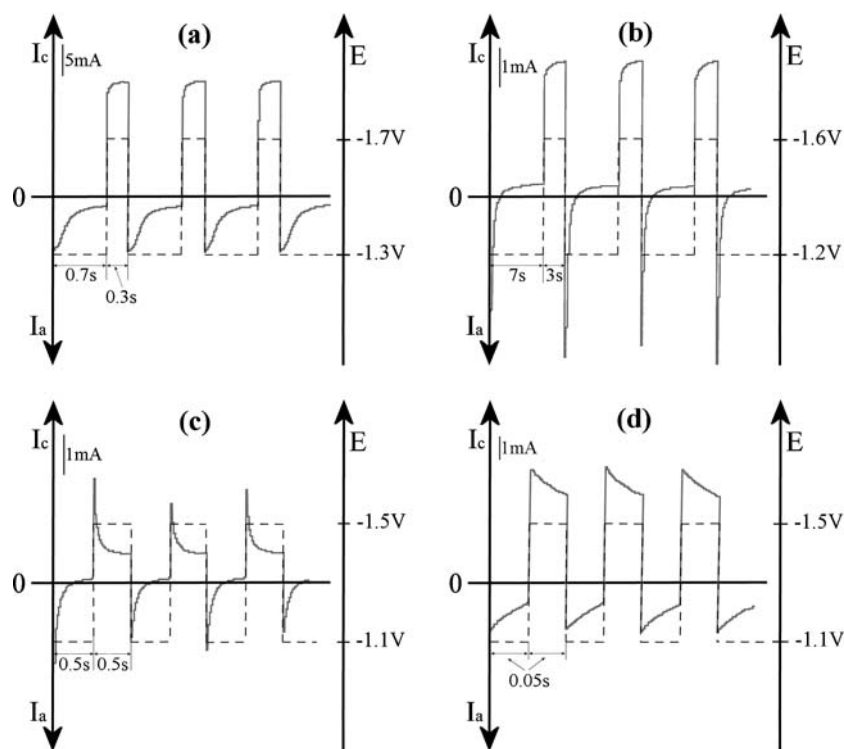


Fig. 2. Applied periodic waveforms of cathodic potential (E: dashed line) and recorded current densities [ $I_a$  (anodic),  $I_c$  (cathodic); continuous line]. The employed pulse frequencies and duty cycles are: (a) 1 Hz, d.c. = 30%; (b) 0.1 Hz, d.c. = 30%; (c) 1 Hz, d.c. = 50%; (d) 10 Hz, d.c. = 50%. Bath composition:  $0.2\text{ M}$   $\text{ZnSO}_4$ ,  $\text{pH} = 3$  and  $0.05 \times 10^{-3}\text{ M}$  (a), (c), (d) or  $0.5 \times 10^{-3}\text{ M}$  in  $\text{SeO}_2$  (b).

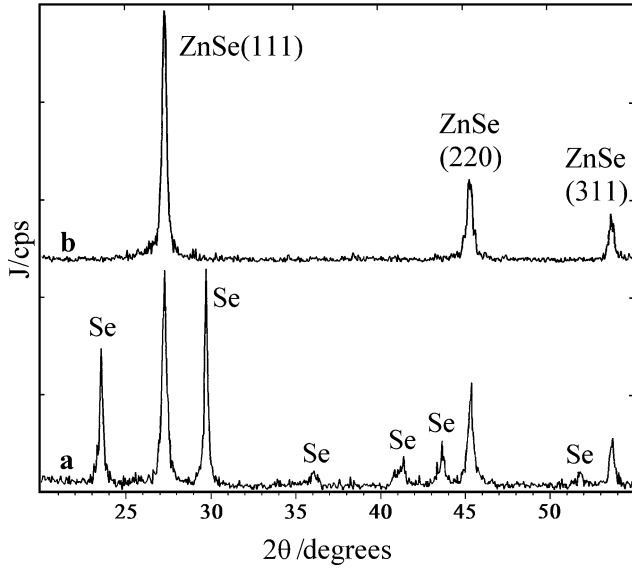


Fig. 3. XRD patterns of a deposit prepared on Ti at  $-1.5/-1.1$  V, 1 Hz, d.c. = 30%, from a  $0.5 \times 10^{-3}$  M  $\text{SeO}_2$ , 0.2 M  $\text{ZnSO}_4$ , pH = 3 solution (a) as-deposited and (b) annealed at  $200^\circ\text{C}$  in air for 30 min.

The layers grown on Ni substrate were of lower crystallinity and less adherent than those grown on Ti, mostly due to the enhanced inhibition that the evolution

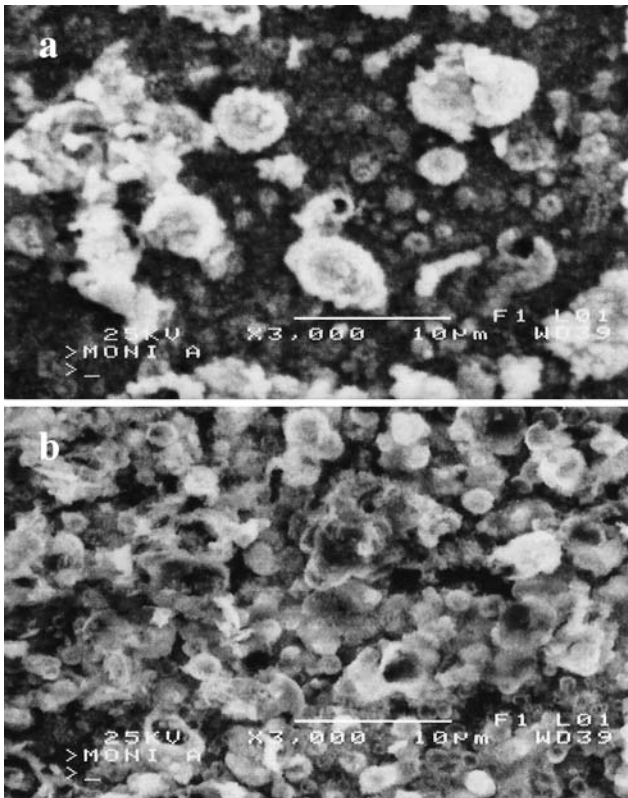


Fig. 4. SEM micrographs of deposits prepared on Ti at  $-1.5/-1.1$  V, 1 Hz, d.c. = 30%, from a  $0.5 \times 10^{-3}$  M  $\text{SeO}_2$ , 0.2 M  $\text{ZnSO}_4$ , pH = 3 solution (a) as-deposited and (b) after heat treatment at  $200^\circ\text{C}$  in air for 30 min. Average atomic composition from EDAX: (a) 26% Zn, 74% Se; (b) 43% Zn, 57% Se.

of hydrogen induces with the Ni cathode at the working potentials. The results for various bias profiles applied to solutions of  $0.05 \times 10^{-3}$  M in  $\text{SeO}_2$  and Ti working electrodes are broadly summarized below. Note that a series of experiments with Ni presented similar features.

- (i) If the more negative potential of the plating cycle is located within the diffusion plateau and its conjugate is more anodic than the plateau onset, then the majority phase obtained is hexagonal Se rather than ZnSe (Figure 5a). In particular, the less negative the “anodic” potential the higher is the Se to ZnSe mass ratio.
- (ii) When both potentials of the cycle lie within the diffusion plateau, rich in zinc-blend ZnSe electrodeposits are formed with an admixture of hexagonal Se. Best results are obtained when the difference of the cycle potentials is large (400–500 mV); adjusting the one potential at the end and the other in the beginning of the plateau turns out to be the best combination (Figure 5b).
- (iii) If the “cathodic” potential lies deep in the overpotential region of Zn (100–300 mV) and the “anodic” one lies at the diffusion plateau, within the underpotential region of Zn, the obtained layers contain mainly Zn (Figure 5c, d). Decreasing the cathodic potential (Figure 5, from d to c) yields comparable quantities of single Zn and Se phases in the deposit.
- (iv) If both the applied potentials are more negative than  $-1.4$  V, i.e. virtually lie in the overpotential region of  $\text{Zn}/\text{Zn}^{2+}$  redox value, the obtained layers consist mainly of metallic Zn (Figure 5e).

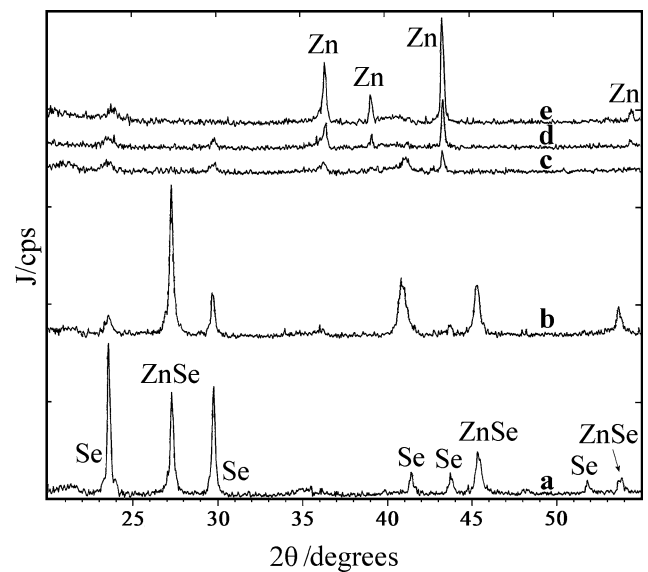


Fig. 5. XRD patterns of equally thick deposits prepared on Ti at various potentials from a  $0.05 \times 10^{-3}$  M  $\text{SeO}_2$ , 0.2 M  $\text{ZnSO}_4$ , pH = 3 solution: (a)  $-1.4/-1.0$  V, (b)  $-1.5/-1.1$  V (c)  $-1.6/-1.2$  V (d)  $-1.7/-1.3$  V (e)  $-1.8/-1.4$  V. The pulse parameters were 1 Hz, d.c. = 30%.

It turns out that the potential profile described in (ii) (Figure 5b) is the choice of preference for the specified conditions.

### 3.3. Effect of pulse plating parameters

The average electrolytic current for the employed conditions was generally constant with time during deposition. However, during a single pulse the current response was more or less distorted from the rectangular form (Figure 2). The best deposits were obtained when enough time was provided for the current to obtain its steady state value. In those cases, a high current was observed in the beginning of a cathodic period, which sharply decreased to a constant diffusion-limited value (Figure 2c) as the concentration of reducing species at the electrode surface dropped to a minimum. Part of the current peak in Figure 2c is the capacitive component. In general, if the charging time of the electric double layer at the cathode interface is longer than the duration of the pulse, the faradaic current corresponding to the applied potential is not reached. The same is true for the anodic current during the discharge stage. Thus, the time length of a pulse plays a major role in establishing an efficient electrolysis regime.

The influence of frequency is illustrated in Figure 6 for a duty cycle of 50% and a selected voltage profile referring to the case (ii) above. For low cycle frequency, i.e. 0.1 Hz (10 s for each potential pulse), Zn and Se elemental phases were preferentially deposited, and ZnSe was not detected at all by XRD. The situation was much improved in the range 1–10 Hz (1–0.1 s pulse). When the frequency exceeded 10 Hz the film quality declined, since too short pulses induce a strong capacitive effect. In this case, the faradaic current

oscillates around an average value, which is less cathodic than the nominal value corresponding to the applied potential, thus resembling a constant current deposition. Thereafter, the XRD diagrams for 1 and 100 Hz in Figure 6 roughly depict the difference between the optimized PPE and the DC deposition, i.e. they demonstrate the amelioration attained when pulsing the potential.

The applied method provided the possibility to diminish the single phase Se atom content of the electrodeposits to 10% in average. In this result, the effect of the duty cycle variation is also taken into account. On the basis of XRD investigation for a  $-1.5/-1.1$  V, 1 Hz profile and for various duty cycles (Figure 7), it turned out that optimal composition was attained at d.c. = 50% value. Thus, Figure 7 shows that the results are getting better by increasing the relative duration of the lower potential from 10 to about 50%. This is valid for either  $0.5$  or  $0.05 \times 10^{-3}$  M  $\text{SeO}_2$  concentrations.

By defining time-averaged values of deposition potential for PPE and assuming similar efficiency of electrolysis for either potentiostatic or pulse plating, on the basis of gravimetric and optical (SEM) density measurements, it was possible to compare electrodeposits obtained by the different plating methods. For similar bath composition and electrolysis charge, pulse plating was found to provide a definite improvement in terms of ZnSe crystallinity and Se excess reduction, at least for working baths of  $0.5 \times 10^{-3}$  M in  $\text{SeO}_2$ . Moreover, the deposition time was significantly diminished (up to 60%). For instance, the attained faradaic charge after 1 h and 30 min operation with a  $-1.1/-1.5$  V, 1 Hz, 30% profile in a  $0.5 \times 10^{-3}$  M  $\text{SeO}_2$  bath was similar to the charge attained after 3 h

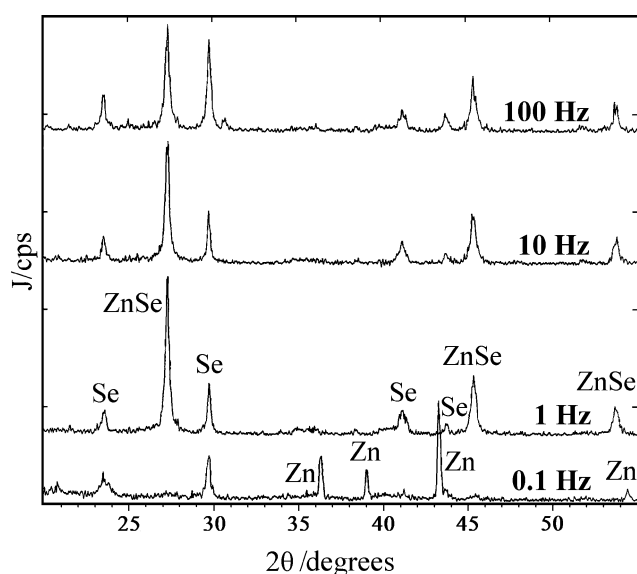


Fig. 6. XRD patterns of equally thick deposits prepared on Ti at  $-1.5/-1.1$  V from a  $0.05 \times 10^{-3}$  M  $\text{SeO}_2$ , 0.2 M  $\text{ZnSO}_4$ , pH = 3 solution, for various frequencies (d.c. = 50%).

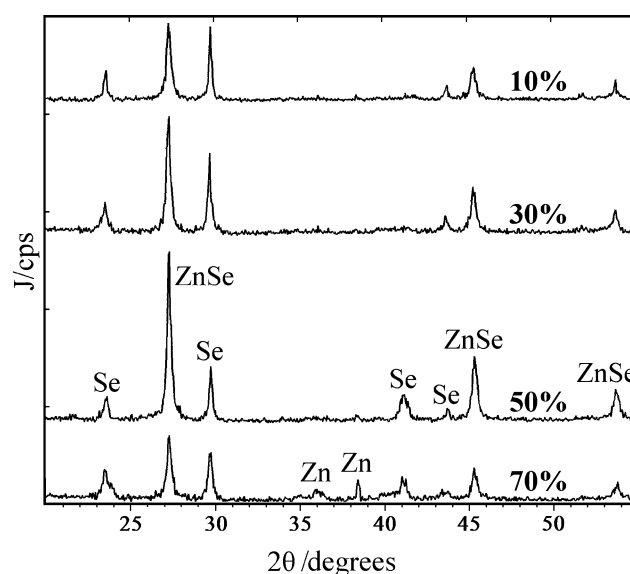


Fig. 7. XRD patterns of equally thick deposits prepared on Ti at  $-1.5/-1.1$  V from a  $0.05 \times 10^{-3}$  M  $\text{SeO}_2$ , 0.2 M  $\text{ZnSO}_4$ , pH = 3 solution, for various duty cycles (frequency: 1 Hz).

30' of potentiostatic deposition at  $-1.2$  V. The respective deposition times in a  $0.05 \times 10^{-3}$  M  $\text{SeO}_2$  bath were about 2 h 30' for PCP and 6 h for DCP.

Pulse plating is possibly the key technique for the electrolytic production of high quality single phase films of the binary compound. The above results arose from a systematic investigation of the parameters involved, while the process might be optimized further by a statistically planned series of experiments, taking into consideration the interplay between all the electrical, hydrodynamical, geometrical and compositional parameters of the bath.

#### 4. Conclusions

Polycrystalline thin films of randomly oriented zinc-blend ZnSe were formed on metallic cathodes from acidic aqueous solutions of selenite and zinc sulphate by pulsed potential electrodeposition comprising an alternating signal of cathodic potential. The magnitude and the time period fraction of each pulse determined the composition of the films in ZnSe, Zn and Se phases. Maximizing the content of crystalline ZnSe, while retaining a low chalcogen excess in the solid, was possible by ensuring a reversing current density response consisting of a diffusion-limited cathodic component, under e.g. a  $[-1.1$  V (0.3–0.5 s)]/ $[-1.5$  V (0.5–0.7 s)] profile (potentials vs. SSE). The applied method allowed higher rate of electrodeposition with better composition control, compared to the potentiostatic process.

#### References

1. T. Niina, K. Yoneda and T. Toda, *J. Electrochem. Soc.* **130** (1983) 2099.
2. C.C. Chang and C.H. Lee, *Thin Solid Films* **379** (2000) 287.
3. T.L. Chu, S.S. Chu, G. Chen, J. Britt, C. Ferekides and C.Q. Wu, *J. Appl. Phys.* **71** (1992) 3865.
4. C. Natarajan, M. Sharon, C. Lévy-Clément and M. Neumann-Spallart, *Thin Solid Films* **237** (1994) 118.
5. A.P. Samantilleke, M.H. Boyle, J. Young and I.M. Dharmadasa, *J. Mater. Sci.: Mater. Electron.* **9** (1998) 231.
6. D. Gal and G. Hodes, *J. Electrochem. Soc.* **147** (2000) 1825.
7. S. Sanchez, C. Lucas, G.S. Picard, M.R. Bermejo and Y. Castrillejo, *Thin Solid Films* **361–362** (2000) 107.
8. (a) M. Bouroushian, T. Kosanovic, Z. Loizos and N. Spyrellis, *J. Solid State Electr.* **6** (2002) 272; (b) M. Bouroushian and T. Kosanovic, *ibid.* **10** (2006) 223.
9. T. Kosanovic, M. Bouroushian and N. Spyrellis, *Mater. Chem. Phys.* **90** (2005) 148.
10. G. Riveros, D. Lincot, J.F. Guillemoles, R. Henríquez, R. Schrebler, R. Cordova and H. Gomez, *J. Electroanal. Chem.* **558** (2003) 9.
11. R. Henríquez, H. Gomez, G. Riveros, J.F. Guillemoles, M. Froment and D. Lincot, *Electrochem. Solid St.* **7** (2004) C75.
12. N. Ibl, J.Cl. Puipe and H. Angerer, *Surf. Technol.* **6** (1978) 287.
13. J.Cl. Puipe and N. Ibl, *J. Appl. Electrochem.* **10** (1980) 775.
14. J.Y. Wang, D. Balamurugan and D.-T. Chin, *J. Appl. Electrochem.* **22** (1992) 240.
15. G.C. Morris and R.J. Vanderveen, *Sol. Energ. Mat. Sol. C* **30** (1993) 339.
16. S.M. Babu, R. Dhanasekaran and P. Ramasamy, *Thin Solid Films* **202** (1991) 67.
17. S.M. Babu, T. Rajalakshmi, R. Dhanasekaran and P. Ramasamy, *J. Cryst. Growth* **110** (1991) 423.
18. V. Swaminathan and K.R. Murali, *Sol. Energ. Mat. Sol. C* **63** (2000) 207.